Robotica (2001) volume 19, pp. 67–77. Printed in the United Kingdom © 2001 Cambridge University Press

Kinematic design of crab-like legged vehicles

Anmin Liu and David Howard

Aeronautical & Mechanical Engineering, University of Salford, Salford M5 4WT (UK)

(Received in Final Form: May 31, 2000)

SUMMARY

In this paper, the kinematic workspace characteristics of a crab-like legged vehicle are investigated using a 2-D model. The alternative kinematic configurations and their corresponding workspace constraints are discussed, and the vehicle configuration of most interest identified. It is shown that, for constant vehicle body attitude, only two parameters affect the kinematic workspace, foot overlap and thigh length. Analytical methods for calculating the workspace characteristics are presented and, using these methods, the effects of the design geometry on the kinematic workspace are investigated.

KEYWORDS: Kinematic design; Crab-like legged vehicle; 2-D model.

1. INTRODUCTION

Many CLAWAR (CLimbing And WAlking Robots) researchers have concentrated on navigation, gait generation and control, rather than mechanical design. When prototypes have been developed, it has often been assumed that the mechanical design principles are known and the problem is one of applying them. In practice, this is far from the truth, as the performance of existing prototypes testifies. The most common design approach is to copy the geometry of insects and mammals with little or no scientific justification. Although there has been some very good work on leg mechanism design,[1–5] the relationships between leg mechanism design and overall machine layout have been neglected.

In principle, legged vehicle design could be treated as one large design optimisation problem. However, the sheer number of parameters and the difficulty of defining a sensible objective function make this approach impractical. In previous work, the authors have divided the walking machine design problem into overall machine design and leg design.[6–8] During overall machine design, the legs are treated as black-boxes which provide the required ground reactions at the feet and have the required kinematic properties. One output of the overall machine design stage is a leg design specification, which then allows the design of an appropriate leg mechanism. The disadvantage of this approach is that it cannot guarantee an optimal design because of the way in which the two design sub-problems have been decoupled.

In this paper, the kinematic design of crab-like walkers and climbers is considered. The design is considered as a whole with no artificial decoupling of leg geometry and overall machine geometry. Crab-like machines represent an important sub-class of multi-legged walkers and climbers.[5] Their importance is a result of their high agility, being particularly well suited to crossing difficult terrains.

Crab-like machines lend themselves to a 2-dimensional analysis because the body and leg movements are almost entirely in the saggital (longitudinal) plane. The body and its supporting legs can be represented by the simple 2-D model shown in Figure 1; note that the non-supporting legs are not shown. The foot spread is equal to $2a$ and the hip spread is equal to $2a_b$. The foot overlap ($s = a–a_b$) is defined as the horizontal distance between the foot and the hip when the vehicle body is in its reference position ($y_b = 0$). The thigh and shank lengths are l_1 and l_2, respectively.

To limit the scope of the study reported here, it was assumed that the vehicle body remains parallel to the ground, and that the ground is flat over the region affecting the vehicle workspace. The kinematic workspace is defined as the region that is accessible to the body-centre without changing the supporting legs. This is a function of the geometry of the legs and the way in which they are constrained by the ground. It is assumed that there are no constraints on the range of rotation of the hip and knee joints. Three workspace characteristics are presented: workspace area; maximum horizontal stroke; and maximum vertical stroke. Note that the terms horizontal and vertical are used for convenience only and refer to movement tangential to and normal to the support surface respectively. Because this study considers kinematic effects only, the orientation of the support surface with respect to the gravity vector is irrelevant.

To simplify the analysis and to generalise the results, all of the dimensions are normalised with respect to the overall leg length. In other words, the overall leg length, l, is taken to be one ($l = l_1 + l_2 = 1$), and all other dimensions are therefore relative to the overall leg length. This means that there is only one independent leg geometry parameter, the thigh length, l_1. Also, for the purposes of the reported work, it will be shown that the body size, a_b, does not affect the kinematic workspace, and that the workspace can be evaluated for all body sizes by considering the case where the body-centre and hip-joints are coincident ($a_b = 0$). Therefore the foot overlap, s, and the thigh length, l_1, are the only independent geometry parameters that influence the kinematic workspace.

2. KINEMATIC CONFIGURATIONS AND CONSTRAINTS

As explained above, to limit the scope of the study reported here, it was assumed that the vehicle body remains parallel

https://doi.org/10.1017/S0263574700002861 Published online by Cambridge University Press

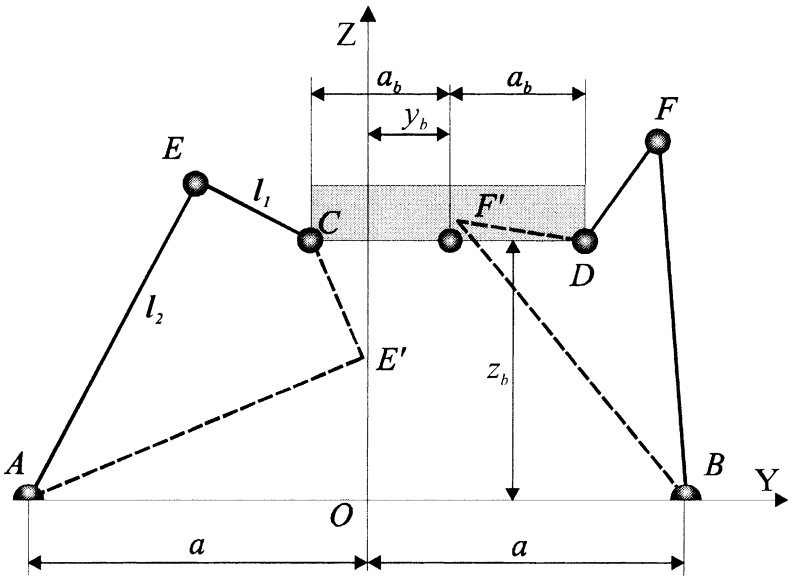

Fig. 1. 2-D model of a crab-like vehicle (non-supporting legs not shown).

to the ground, and that the ground is flat over the region affecting the vehicle workspace. Therefore, the attitude of the vehicle body remains constant, and the body-centre and hip-joints follow parallel paths. This means that, for a given value of foot overlap ($s = a - a_b$), the body size, a_b, does not affect the kinematic workspace, and that the workspace can be evaluated for all body sizes by considering the case where the body-centre and hip-joints are coincident ($a_b = 0$).

Referring to Figure 1, there are eight possible vehicle configurations. Firstly, s (a–a_b) can be either positive or negative. Secondly, in each case, there are four possible configurations of the legs:

- Leg 1 knee-out – Leg 2 knee-out (A-E-C-D-F-B in Figure 1)
- Leg 1 knee-out – Leg 2 knee-in (A-E-C-D-F'-B in Figure 1)
- Leg 1 knee-in – Leg 2 knee-out (A-E'-C-D-F-B in Figure 1)
- Leg 1 knee-in – Leg 2 knee-in (A-E'-C-D-F'-B in Figure 1)

From a kinematic workspace point of view, the second and third configurations are simply mirror images, which reduces the number of relevant leg configurations to three (six vehicle configurations). Because, for kinematic purposes, the body size can be considered to be zero ($a_b = 0$), every configuration where s is negative is equivalent to another configuration where s is positive. This reduces the number of relevant vehicle configurations to the three shown in Figure 2. To visualise the original eight configurations, it is helpful to picture the three cases in Figure 2 with $a_b \neq 0$

For each of the three vehicle configurations, Figure 3 shows the workspace boundaries resulting from the geometry of the legs and the way in which they are constrained by the ground. The upper boundary is symmetrical about the z-axis (located mid way between the two feet) and is a result of one of the legs reaching its fully extended length. For example, on the right hand side of the z-axis, the upper boundary (circle 1) consists of a circle of radius $r_1 = l_1 + l_2 = 1$ and centre $[-s, 0]$, and can be expressed as

$$z_1 = [1 - (y_b + s)^2]^{1/2}$$

When $l_1 < l_2$ ($l_1 < 0.5$) the constraints forming the lower boundary include two circles (circle 2) which are mirror images of one another about the z-axis, and which are a result of the thigh being folded back so that the knee angle is zero. In this case, it is impossible for the hip to move closer to its corresponding foot. For example, on the right hand side of the z-axis, circle 2 has a radius $r_2 = (l_2 - l_1)$ and centre $[s, 0]$, and can be expressed as

$$z_2 = [(r_2)^2 - (y_b - s)^2]^{1/2}$$

The constraints forming the lower boundary also include another two circles (circle 3) which are a result of the shank lying on the ground. In this case, it is impossible for the hip to move closer to the point on the ground where its corresponding knee lies. For example, on the right hand side of the z-axis in configuration 1 (Figure 3a), circle 3 has a radius $r_3 = l_1$ and centre $[s + l_2, 0]$, and can be expressed as

$$z_3 = [(r_3)^2 - (y_b - s - l_2)^2]^{1/2}$$

Note that when $s = 0$ ($a = a_b$), the workspace constraints for configurations 1 and 2 converge. In Figure 3, it has been assumed that the areas between circles that cannot form part of a continuous horizontal motion are of little or no value. Therefore, these areas are referred to as waste areas, and are not included in the useful workspace area.

It is apparent that configuration 2 (Figure 3b), where both legs are in their knee-in configurations, has no advantage from a kinematic workspace perspective. Although configuration 3 (Figure 3c) may have some advantages in particular circumstances, in this paper we concentrate on configuration 1 (Figure 3a) because it is the best configuration if the design is to be optimised for maximum horizontal stroke and it allows the vehicle's body to reach the ground.

https://doi.org/10.1017/S0263574700002861 Published online by Cambridge University Press

3. WORKSPACE ANALYSIS

In this section, configuration 1 is analysed in detail and expressions are developed for the workspace area, *A*, maximum horizontal stroke, *DY*, and maximum vertical stroke, *DZ*. As the workspace is symmetrical about the z-axis, the workspace area can be calculated by integrating the accessible area to the right of the z-axis and doubling that value, thus

$$A = 2\int_0^{y_{b\,\mathrm{lim}}} (z_{b\,\max}(y_b) - z_{b\,\min}(y_b))\,dy_b$$

where $z_{bmax}(y_b)$ and $z_{bmin}(y_b)$ are the upper and lower workspace boundaries, and y_{blim} is the maximum horizontal displacement and corresponds to the point of intersection between the lower boundary and circle 1.

The maximum horizontal stroke is given by

$$DY = 2y_{blim}$$

The maximum vertical stroke always occurs at $y_b = 0$ and is given by

$$DZ = z_{bmax}(0) - z_{bmin}(0)$$

Although $z_{bmax}(y_b)$ is always equal to z_1, the expressions for $z_{bmin}(y_b)$ and y_{blim} depend on the way in which circles 1, 2 and 3 intersect with each other and the z-axis, which in turn depends on the design parameters, s and l_1. The flow charts shown in Figures 4 to 7 determine which of the 13 different cases applies. The logical conditions contained in those flow charts require knowledge of the following intersection points (when they exist):

a) the point of intersection of circles 1 and 2

$$y_{12} = (1 - \mathrm{l}_\mathrm{l})l_l/s$$
$$z_{12} = [1 - (y_{12} + s)^2]^{1/2}$$

b) the point of intersection of circles 1 and 3

$$y_{13} = l_2(1 + \mathrm{s})/(2s + l_2)$$
$$z_{13} = [1 - (y_{13} + s)^2]^{1/2}$$

c) the point of intersection of circle 1 and the horizontal line $z = r_2$

$$y_{1r2} = -s + 2(l_1 l_2)^{1/2}$$
$$z_{1r2} = r_2$$

d) the point of intersection of circle 3 and the horizontal line $z = r_2$

$$y_{3r2} = s + l_2 - [2l_1 l_2 - l_2^2]^{1/2}$$
$$z_{3r2} = r_2$$

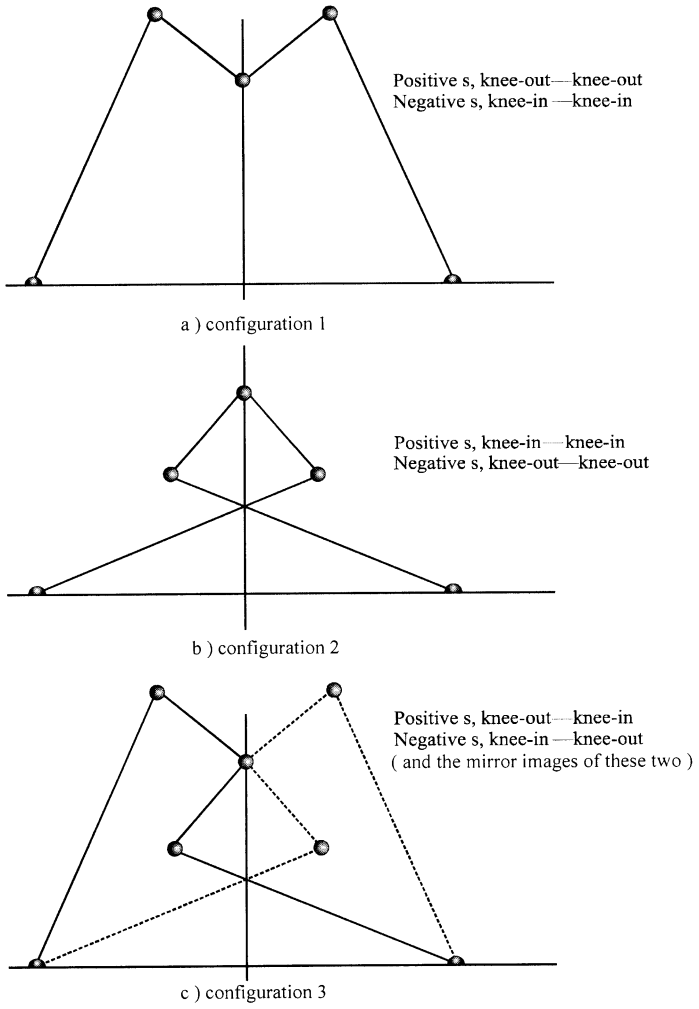

Fig. 2. Vehicle configurations.

https://doi.org/10.1017/S0263574700002861 Published online by Cambridge University Press

e) the point of intersection of circle 1 and the horizontal line $z = r_3$

$$y_{1r3} = [l - l_1^2]^{1/2} - s$$

$$z_{1r3} = r_3$$

The 13 different cases that determine the lower workspace boundary are now described. The logical conditions leading to each case are explained, and expressions are given for $z_{bmax}(y_b)$, $z_{bmin}(y_b)$ and y_{blim}. There are four main cases corresponding to Figures 4 to 7, which then break down into 13 sub-cases.

3.1 Case 1: no part of circle 2 or circle 3 is within circle 1 (Figure 4)

In this case, no part of circle 2 or circle 3 is within circle 1. The logical conditions leading to this case are as follows:

either $l_1 < 0.5$ *and* $s \geq l_2$

or $l_1 \geq 0.5$ *and* $s \geq l_1$

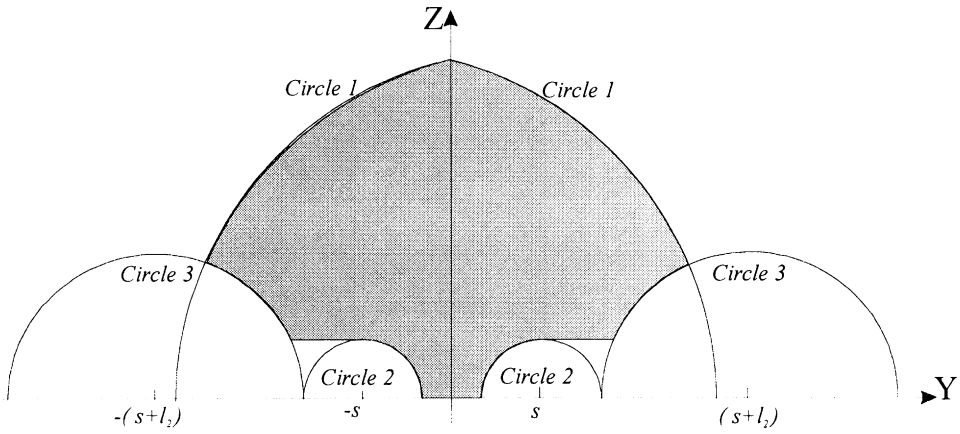

a) the workspace of configuration 1

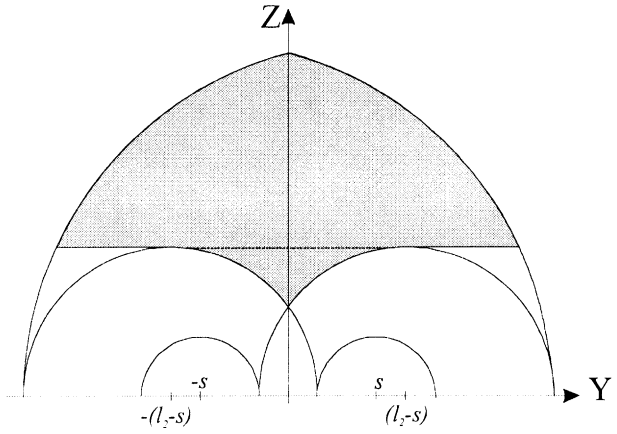

b) the workspace of configuration 2

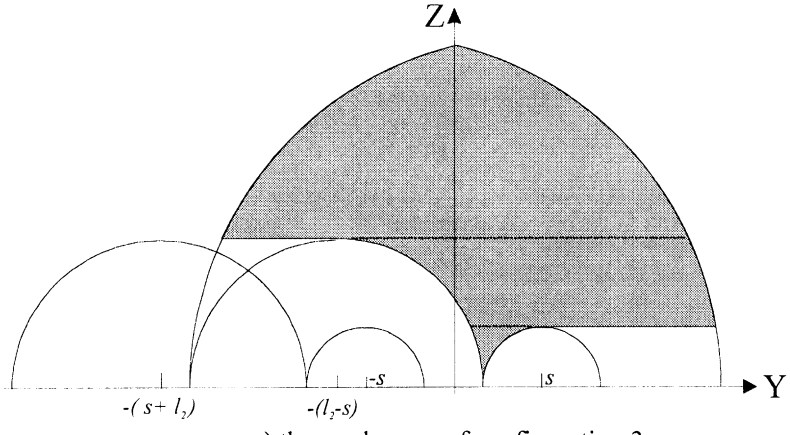

c) the workspace of configuration 3

Fig. 3. Workspace boundaries.

https://doi.org/10.1017/S0263574700002861 Published online by Cambridge University Press

When the first condition applies, both circle 2 and circle 3 exist, and they are both outside circle 1. When the second condition applies, circle 2 does not exist, and circle 3 is outside circle 1.

In this case, the upper boundary, lower boundary and horizontal limit of the workspace are given by:

$$z_{b\,\max} = z_1$$
$$z_{b\,\min} = 0$$
$$y_{b\,\lim} = 1 - s$$

3.2 Case 2: part or all of circle 2 is within circle 1 (Figure 5)

In this case, part or all of circle 2 is within circle 1, and circle 3 is outside circle 1. The logical condition leading to this case is as follows:

$$l_1 < 0.5 \text{ and } l_1 \le s < l_2$$

The three components of this logical condition mean that circle 2 exists, circle 3 is outside circle 1, and part or all of circle 2 is within circle 1 respectively. Referring to Figure 5, this case divides into four sub-cases as follows.

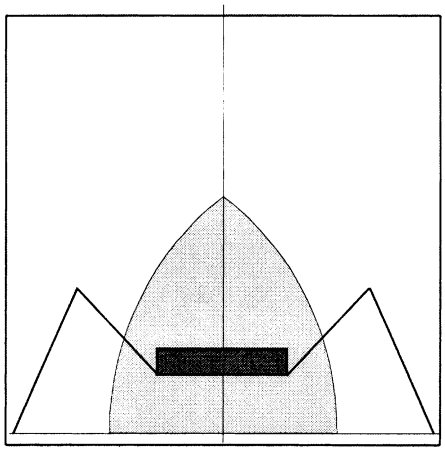

Fig. 4. Case 1: no part of circle 2 or circle 3 is within circle 1.

Sub-case 2.1. In this sub-case, circle 2 intersects with the z-axis (centre-line) and there is a waste area due to circle 2. The logical condition leading to this sub-case is as follows:

$$s \le r_2 \text{ and } s < y_{12}$$

In this case, the upper boundary, lower boundary and horizontal limit of the workspace are given by:

$$z_{b\,\max} = z_1$$

$$z_{b\,\min} = \begin{cases} z_2 & 0 \le y_b \le s \\ r_2 & s < y_b \le y_{1r2} \end{cases}$$

$$y_{b\,\lim} = y_{1r2}$$

Sub-case 2.2. In this sub-case, circle 2 intersects with the z-axis (centre-line) and there is *not* a waste area due to circle 2. The logical condition leading to this sub-case is as follows:

$$s \le r_2 \text{ and } s \ge y_{12}$$

In this case, the upper boundary, lower boundary and horizontal limit of the workspace are given by:

$$z_{b\,\max} = z_1$$
$$z_{b\,\min} = z_2$$
$$y_{b\,\lim} = y_{12}$$

Sub-case 2.3. In this sub-case, circle 2 does *not* intersect with the z-axis (centre-line) and there is a waste area due to circle 2. The logical condition leading to this sub-case is as follows:

$$s > r_2 \text{ and } s < y_{12}$$

In this case, the upper boundary, lower boundary and horizontal limit of the workspace are given by:

$$z_{b\,\max} = z_1$$

$$z_{b\,\min} = \begin{cases} 0 & 0 \le y_b \le s - r_2 \\ z_2 & s - r_2 < y_b \le s \\ r_2 & s < y_b \le y_{1r2} \end{cases}$$

$$y_{b\,\lim} = y_{1r2}$$

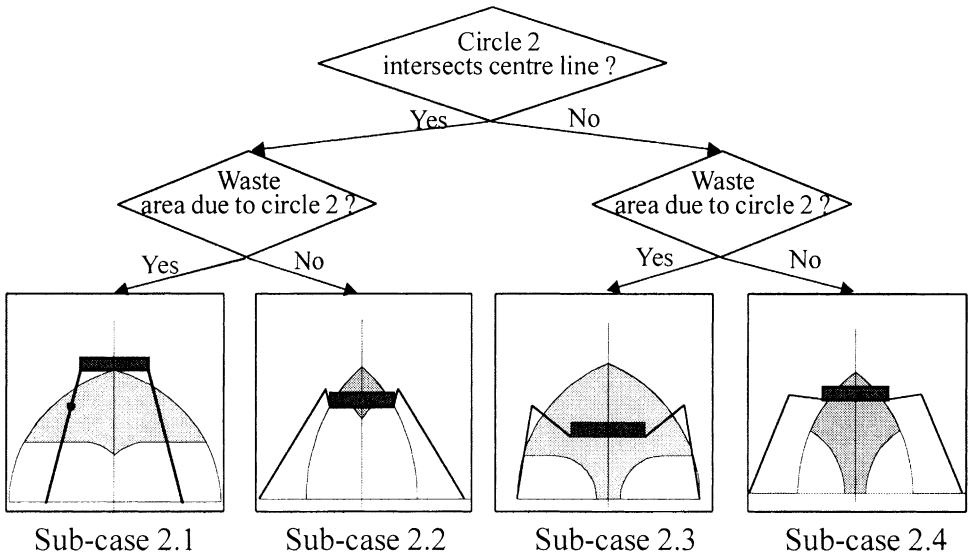

Fig. 5. Case 2: part or all of circle 2 is within circle 1.

https://doi.org/10.1017/S0263574700002861 Published online by Cambridge University Press

Sub-case 2.4. In this sub-case, circle 2 does *not* intersect with the z-axis (centre-line) and there is *not* a waste area due to circle 2. The logical condition leading to this sub-case is as follows:

$$s > r_2 \text{ and } s \geq y_{12}$$

In this case, the upper boundary, lower boundary and horizontal limit of the workspace are given by:

$$z_{b\,\max} = z_1$$

$$z_{b\,\min} = \begin{cases} 0 & 0 \leq y_b \leq s - r_2 \\ z_2 & s - r_2 < y_b \leq y_{12} \end{cases}$$

$$y_{b\,\lim} = y_{12}$$

3.3 Case 3: part or all of circle 3 is within circle 1 (Figure 6)

In this case, circle 2 does not exist, and part or all of circle 3 is within circle 1. The logical condition leading to this case is as follows:

$$l_1 \geq 0.5 \text{ and } s < l_1$$

Referring to Figure 6, this case divides into four sub-cases as follows.

Sub-case 3.1. In this sub-case, circle 3 intersects with the z-axis (centre-line) and there is a waste area due to circle 3. The logical condition leading to this sub-case is as follows:

$$s \leq -r_2 \text{ and } s + l_2 < y_{13}$$

In this case, the upper boundary, lower boundary and horizontal limit of the workspace are given by:

$$z_{b\,\max} = z_1$$

$$z_{b\,\min} = \begin{cases} z_3 & 0 \leq y_b \leq s + l_2 \\ r_3 & s + l_2 < y_b \leq y_{1r3} \end{cases}$$

$$y_{b\,\lim} = y_{1r3}$$

Sub-case 3.2 In this sub-case, circle 3 intersects with the z-axis (centre-line) and there is *not* a waste area due to circle 3. The logical condition leading to this sub-case is as follows:

$$s \leq -r_2 \text{ and } s + l_2 \geq y_{13}$$

In this case, the upper boundary, lower boundary and horizontal limit of the workspace are given by:

$$z_{b\,\max} = z_1$$

$$z_{b\,\min} = z_3$$

$$y_{b\,\lim} = y_{13}$$

Sub-case 3.3. In this sub-case, circle 3 does *not* intersect with the z-axis (centre-line) and there is a waste area due to circle 3. The logical condition leading to this sub-case is as follows:

$$s > -r_2 \text{ and } s + l_2 < y_{13}$$

In this case, the upper boundary, lower boundary and horizontal limit of the workspace are given by:

$$z_{b\,\max} = z_1$$

$$z_{b\,\min} = \begin{cases} 0 & 0 \leq y_b \leq s + r_2 \\ z_3 & s + r_2 < y_b \leq s + l_2 \\ r_3 & s + l_2 < y_b \leq y_{1r3} \end{cases}$$

$$y_{b\,\lim} = y_{1r3}$$

Sub-case 3.4. In this sub-case, circle 3 does *not* intersect with the z-axis (centre-line) and there is *not* a waste area due to circle 3. The logical condition leading to this sub-case is as follows:

$$s > -r_2 \text{ and } s + l_2 \geq y_{13}$$

In this case, the upper boundary, lower boundary and horizontal limit of the workspace are given by:

$$z_{b\,\max} = z_1$$

$$z_{b\,\min} = \begin{cases} 0 & 0 \leq y_b \leq s + r_2 \\ z_3 & s + r_2 < y_b \leq y_{13} \end{cases}$$

$$y_{b\,\lim} = y_{13}$$

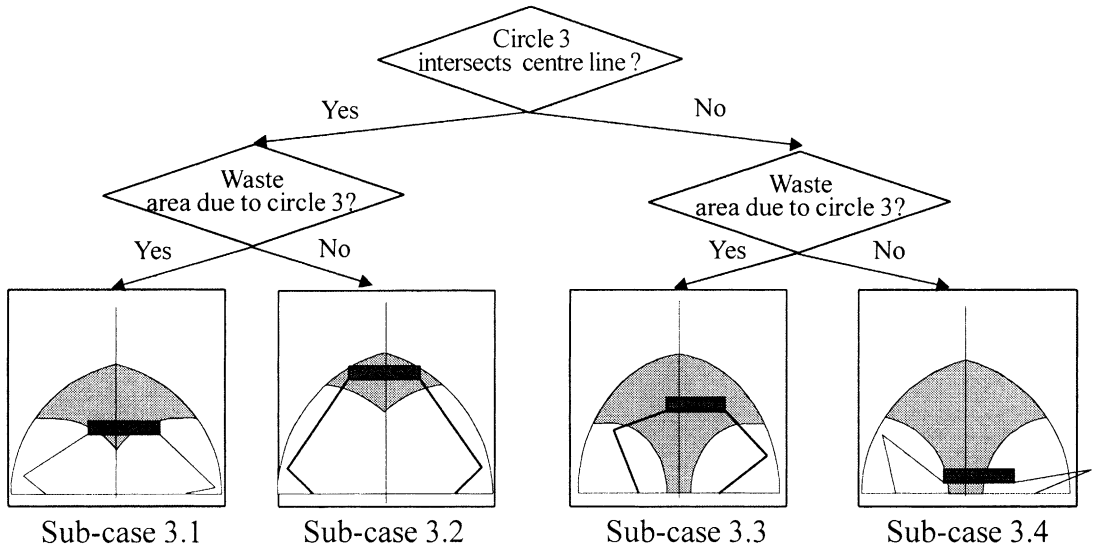

Fig. 6. Case 3: part or all of circle 3 is within circle 1.

https://doi.org/10.1017/S0263574700002861 Published online by Cambridge University Press

3.4 Case 4: circle 2 and part or all of circle 3 are within circle 1 (Figure 7)

In this case, circle 2 is entirely within circle 1, and part or all of circle 3 is within circle 1. The logical condition leading to this case is as follows:

$$l_1 < 0.5 \text{ and } s < l_1$$

The first component of the logical condition means that circle 2 exists, and the second component means that part or all of circle 3 is within circle 1. Referring to Figure 7, this case divides into six sub-cases, two of which correspond to sub-cases 2.1 and 2.3 above.

Sub-case 4.1. In this sub-case, circle 3 is lower than circle 2 when $y_b \leq y_{b\,\mathrm{lim}}$, therefore circle 3 has no effect on the workspace. Also, circle 2 intersects with the z-axis (centre-line). Two logical conditions lead to this case, they are as follows:

If	$s + l_2 < y_{13}$
then	$r_3 \leq r_2$ *and* $s \leq r_2$
else	$z_{13} \leq r_2$ *and* $s \leq r_2$

In the first case, the centre of circle 3 is nearer the origin than the point of intersection between circles 1 and 3 (there is a waste area due to circle 3). Therefore, the radius of circle 3 must be less than the radius of circle 2. In the second case, the point of intersection between circles 1 and 3 is nearer the origin than the centre of circle 3 (there is no waste area due to circle 3). Therefore, the point of intersection between circles 1 and 3 must be lower than circle 2.

Because circle 3 has no effect on the workspace, this sub-case is the same as sub-case 2.1, and therefore the upper boundary, lower boundary and horizontal limit of the workspace are given by the equations for sub-case 2.1.

Sub-case 4.2. In this sub-case, circle 3 is lower than circle 2 when $y_b \leq y_{b\,\mathrm{lim}}$, therefore circle 3 has no effect on the workspace. Also, circle 2 does *not* intersect with the z-axis (centre-line). Two logical conditions lead to this case, they are as follows:

If	$s + l_2 < y_{13}$
then	$r_3 \leq r_2$ *and* $s > r_2$
else	$z_{13} \leq r_2$ *and* $s > r_2$

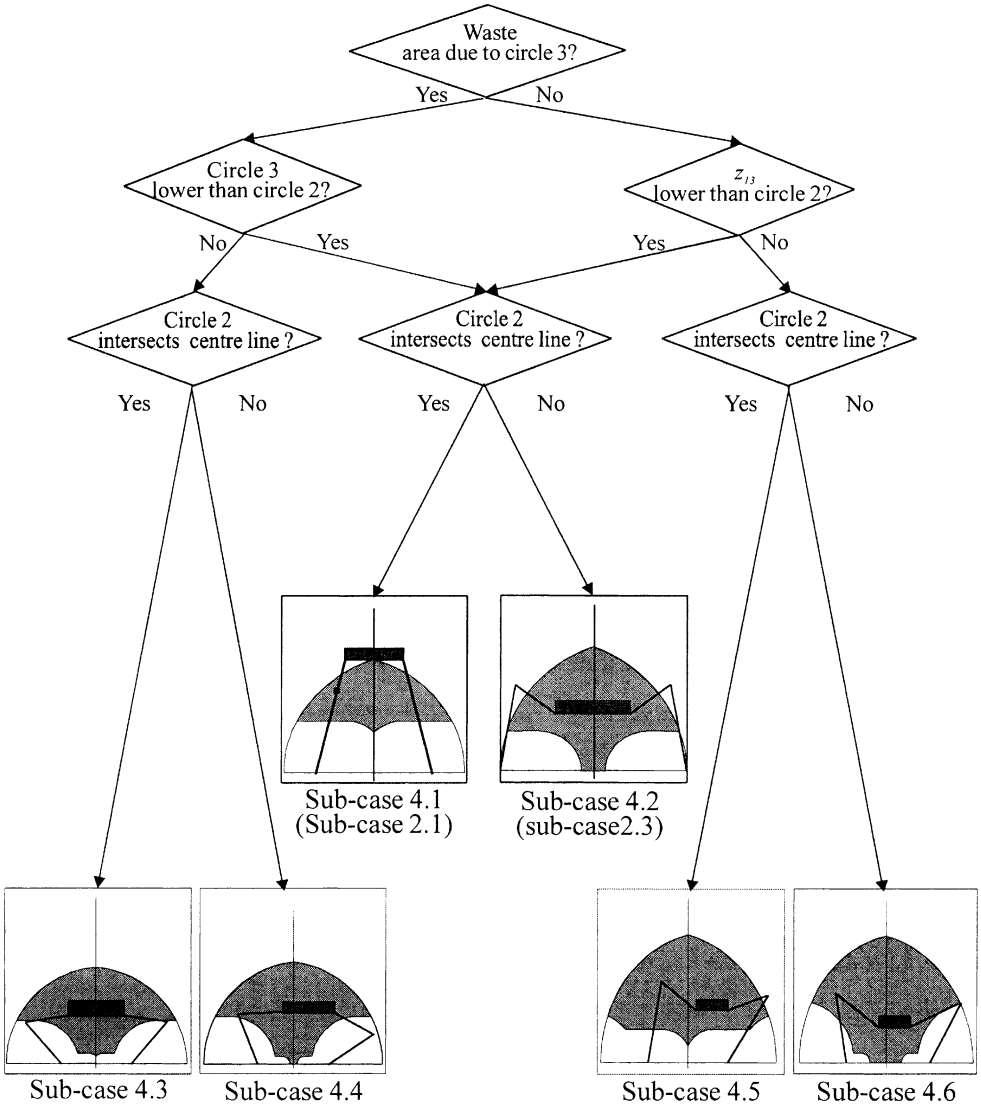

Fig. 7. Case 4: circle 2 and part or all of circle 3 are within circle 1.

https://doi.org/10.1017/S0263574700002861 Published online by Cambridge University Press

In the first case, the centre of circle 3 is nearer the origin than the point of intersection between circles 1 and 3 (there is a waste area due to circle 3). Therefore, the radius of circle 3 must be less than the radius of circle 2. In the second case, the point of intersection between circles 1 and 3 is nearer the origin than the centre of circle 3 (there is no waste area due to circle 3). Therefore, the point of intersection between circles 1 and 3 must be lower than circle 2.

Because circle 3 has no effect on the workspace, this sub-case is the same as sub-case 2.3, and therefore the upper boundary, lower boundary and horizontal limit of the workspace are given by the equations for sub-case 2.3.

Sub-case 4.3. In this sub-case, there is a waste area due to circle 3, circle 3 is higher than circle 2, and circle 2 intersects with the z-axis. The logical condition leading to this case is as follows:

$$s + l_2 < y_{13} \; and \; r_3 > r_2 \; and \; s \le r_2$$

In this case, the upper boundary, lower boundary and horizontal limit of the workspace are given by:

$$z_{b\,\max} = z_1$$

$$z_{b\,\min} = \begin{cases} z_2 & 0 \le y_b \le s \\ r_2 & s < y_b \le y_{3r2} \\ z_3 & y_{3r2} < y_b \le s + l_2 \\ r_3 & s + l_2 < y_b \le y_{1r3} \end{cases}$$

$$y_{b\,\lim} = y_{1r3}$$

Sub-case 4.4. In this sub-case, there is a waste area due to circle 3, circle 3 is higher than circle 2, and circle 2 does *not* intersect with the z-axis. The logical condition leading to this case is as follows:

$$s + l_2 < y_{13} \; and \; r_3 > r_2 \; and \; s > r_2$$

In this case, the upper boundary, lower boundary and horizontal limit of the workspace are given by:

$$z_{b\,\max} = z_1$$

$$z_{b\,\min} = \begin{cases} 0 & 0 \le y_b \le s - r_2 \\ z_2 & s - r_2 < y_b \le s \\ r_2 & s < y_b \le y_{3r2} \\ z_3 & y_{3r2} < y_b \le s + l_2 \\ r_3 & s + l_2 < y_b \le y_{1r3} \end{cases}$$

$$y_{b\,\lim} = y_{1r3}$$

Sub-case 4.5. In this sub-case, there is *not* a waste area due to circle 3, circle 3 is higher than circle 2, and circle 2 intersects with the z-axis. The logical condition leading to this case is as follows:

$$s + l_2 \ge y_{13} \; and \; z_{13} > r_2 \; and \; s \le r_2$$

In this case, the upper boundary, lower boundary and horizontal limit of the workspace are given by:

$$z_{b\,\max} = z_1$$

$$z_{b\,\min} = \begin{cases} z_2 & 0 \le y_b \le s \\ r_2 & s < y_b \le y_{3r2} \\ z_3 & y_{3r2} < y_b \le y_{13} \end{cases}$$

$$y_{b\,\lim} = y_{13}$$

Sub-case 4.6. In this sub-case, there is *not* a waste area due to circle 3, circle 3 is higher than circle 2, and circle 2 does *not* intersect with the z-axis. The logical condition leading to this case is as follows:

$$s + l_2 \ge y_{13} \; and \; z_{13} > r_2 \; and \; s > r_2$$

In this case, the upper boundary, lower boundary and horizontal limit of the workspace are given by:

$$z_{b\,\max} = z_1$$

$$z_{b\,\min} = \begin{cases} 0 & 0 \le y_b \le s - r_2 \\ z_2 & s - r_2 < y_b \le s \\ r_2 & s < y_b \le y_{3r2} \\ z_3 & y_{3r2} < y_b \le y_{13} \end{cases}$$

$$y_{b\,\lim} = y_{13}$$

4. THE INFLUENCE OF THE DESIGN PARAMETERS (*s* AND l_1) ON KINEMATIC WORKSPACE

The analysis presented in the previous section has been incorporated in a MATLAB program which was subsequently used to produce the design maps presented in Figures 8 to 10. As already explained, because the attitude of the vehicle body remains constant, the kinematic workspace is a function of the foot overlap ($s = a – a_b$) and thigh length (l_1) only. Various features of the curves presented can be explained by consideration of the geometry of Figures 1 to 3.

The extreme cases where $l_1 = 0$ and $l_1 = 1$ can be understood by consideration of Figure 1. In both cases the leg becomes a single link connecting the hip to the foot and the machine reduces to the equivalent of a 4-bar chain. Therefore, the workspace collapses onto a single line (the coupler-curve), and hence the workspace area, maximum horizontal stroke, and maximum vertical stroke are all zero.

It is also clear that increasing foot overlap, *s*, reduces the useful workspace in all three respects. This is because the vehicle workspace consists of the intersection of the two workspaces allowed by each leg acting alone. When $s = 0$, with the exception of the two circles caused by the shanks lying on the ground (circle 3), the workspace constraints due to the two legs coincide. Therefore the reduction in workspace as a result of having two legs rather than one is at a minimum. As *s* is increased, the constraints due to the two legs diverge and the useful workspace reduces.

The straight-line segments in Figures 8b and 9b coincide with Case 1 (see section 3.1), where no part of circle 2 or circle 3 is within circle 1, and hence l_1 has no effect on workspace area or maximum horizontal stroke. The straight-line segments in Figure 10b correspond to the cases where neither circle 2 nor circle 3 intersect with the centre-line (z-

https://doi.org/10.1017/S0263574700002861 Published online by Cambridge University Press

axis). In this case, the maximum vertical stroke is constrained only by the ground and circle 1, and hence, l_1 has no effect on maximum vertical stroke.

The *greatest* maximum horizontal stroke occurs when $s = 0$ (already explained) and $l_1 = 1/3$. This corresponds to the case where, for $s = 0$, $r_2 = r_3$. Because the height of the maximum horizontal stroke is equal to *max* (r_2, r_3), this logical condition means that the maximum horizontal stroke occurs at the lowest position possible. The *greatest* maximum vertical stroke occurs when $s = 0$ (already explained) and $l_1 = 0.5$. This corresponds to the case where, for $s = 0$, neither circle 2 nor circle 3 intersect with the centre-line (z-axis) and therefore the maximum vertical stroke is constrained only by the ground and circle 1. Although an explicit reason is less apparent, it is not surprising that the maximum workspace area occurs when $s = 0$ and $l_1 = 0.38$, a value which lies between 0.333 and 0.5.

5. CONCLUSIONS

In this paper, the kinematic workspace characteristics of a crab-like legged vehicle have been investigated using the

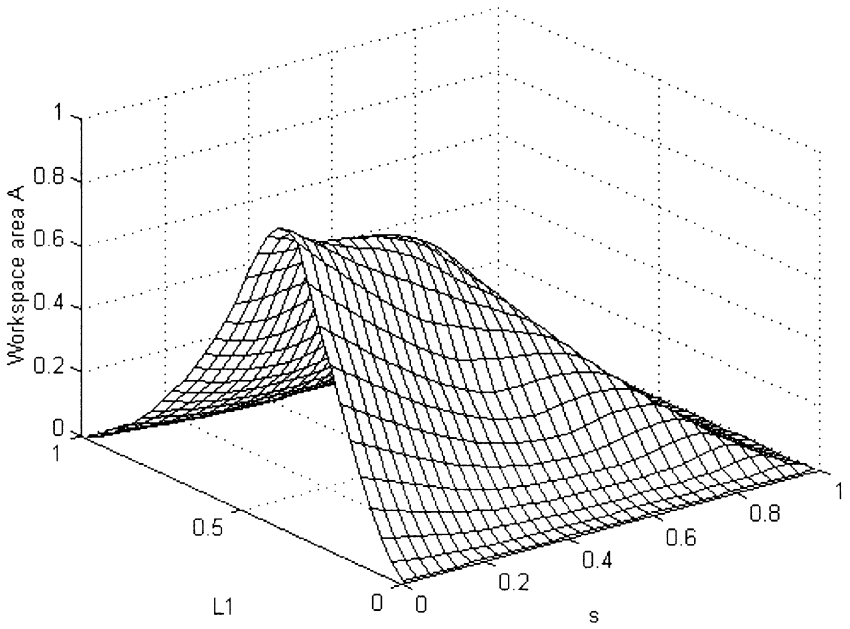

(a)

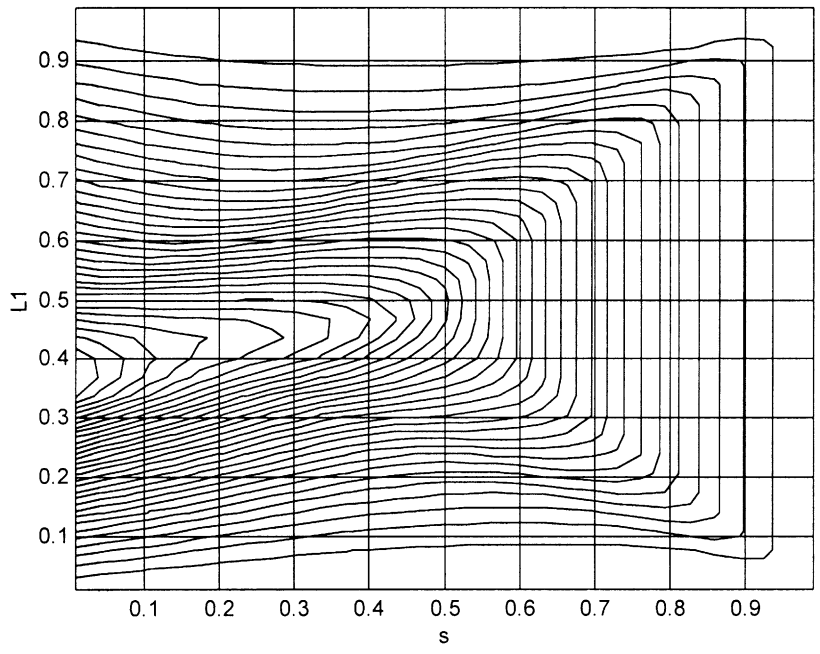

(b)

Fig. 8. Workspace area A vs. l_1 and s.

https://doi.org/10.1017/S0263574700002861 Published online by Cambridge University Press

2-D model described by Figure 1. The alternative kinematic configurations and their corresponding workspace constraints have been discussed, and the vehicle configuration of most interest identified (both legs in their knee-out configurations). It has been shown that, for constant vehicle body attitude, only two parameters affect the kinematic workspace, foot overlap, *s*, and thigh length, l_1. Analytical methods for calculating the workspace characteristics of the chosen configuration were then presented. Using these methods, the effects of the design geometry on the kinematic workspace have been investigated (Figures 8 to 10).

From a purely kinematic point of view the foot overlap, *s*, should be zero ($a_b = a$). However, previous work[7] has shown that a large foot overlap ($a_b << a$) can reduce the installed joint torques required and, hence, the machine weight. So long as the foot overlap is constant, the foot spread, *a*, does not affect the kinematic workspace, however, it obviously has a direct effect on the machine's stability (resistance to tipping over).

For workspace area and maximum horizontal stroke, there are distinct optimum values of thigh length (l_1) when $s < \sim 0.5$. When $s > \sim 0.5$, there is a range of values of thigh length which optimise area or maximum horizontal stroke (see the straight-line segments in Figures 8b and 9b). For maximum vertical stroke and $s = 0$, the optimum thigh length is $l_1 = 0.5$, however, at all other values of *s*, there is a range of values of thigh length which optimise maximum vertical stroke (see the straight-line segments in Figure 10b). Thigh length will also affect the installed knee torque and, hence, the machine weight.[8]

Although joint angles have not been presented, in practice certain types of joint actuator may have rotation range limitations. Once a promising design has been identified from the data provided (Figures 8 to 10), it is a simple matter to calculate the hip-joint and knee-joint angles for particular paths through the workspace and then if necessary to reappraise the design geometry.

In conclusion, although the results presented indicate the effects of machine geometry on kinematic workspace, the

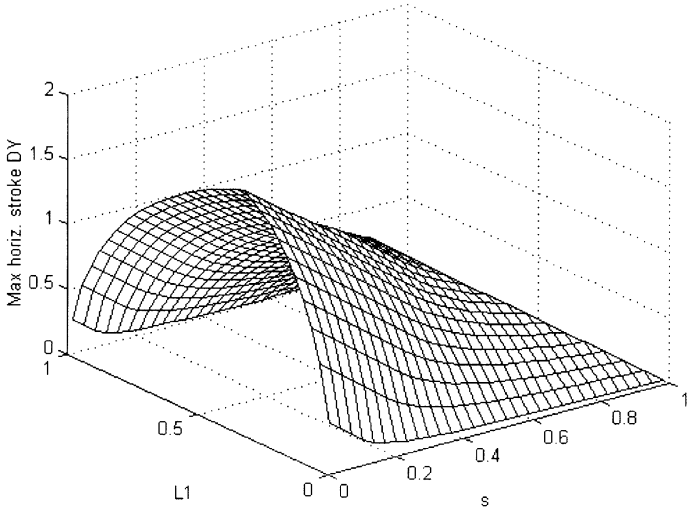

(a)

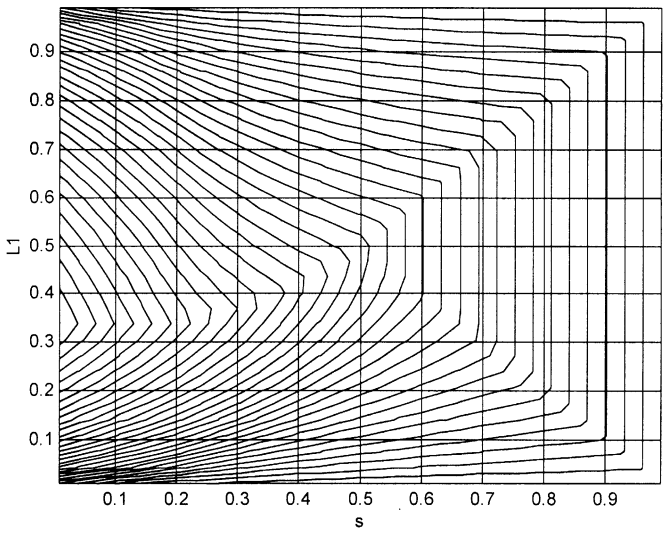

(b)

Fig. 9. Maximum horizontal stroke DY vs. l_1 and *s*.

https://doi.org/10.1017/S0263574700002861 Published online by Cambridge University Press

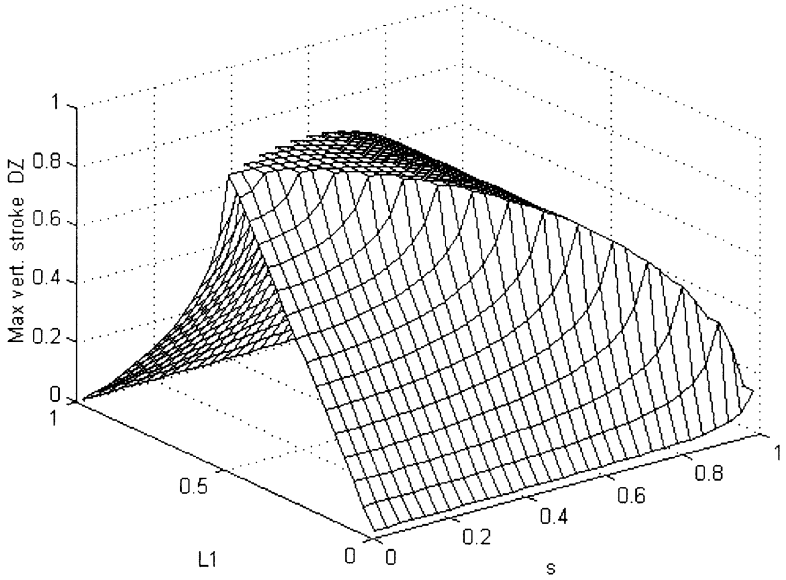

(a)

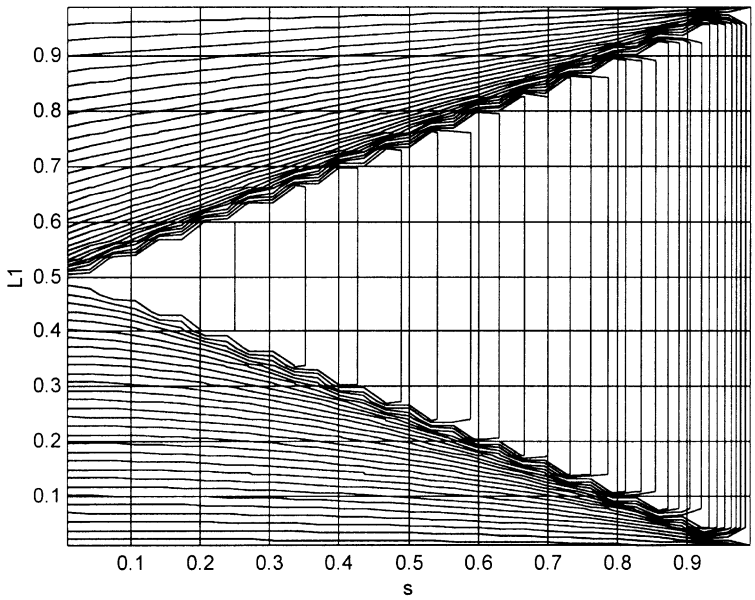

(b)

Fig. 10. Maximum vertical stroke DZ vs. l_1 and s.

design process must also take account of the effects of geometry on machine weight and stability.[6–8]

References

1. S.M. Song, K.J. Waldron and G.L. Kinzel, "Computer-aided Geometric Design of Legs for a Walking Vehicle", *Mechanism and Machine Theory*, **20**, No. 6, 587–596 (1985).
2. M. Kaneko et al, "A Hexapod Walking Vehicle with Decoupled Freedoms", *IEEE Journal of Robotics and Automation* **RA-11**, No. 4, 183–190 (Dec., 1985).
3. S. Dhanadapani and M.M. Ogot, "Modelling of a leg system to illustrate the feasibility of energy recovery in walking machines", *Proc. of 1994 ASME Design Technical Conference*, Minneapolis, Minnesota, (11-14 Sept., 1994) Part 2 (of 2) **Vol. 69–2**, pp. 429–435.
4. W.B. Shieh, L.W. Tsai, S. Azarm and A.L. Tits, "Multi-objective optimisation of a leg mechanism with various spring configurations for force reduction", *Trans. ASME, Journal of Mechanical Design*, **118**, 179–185, (June, 1996)
5. A.M. Liu, and D. Howard, "Leg mechanism designs for CLAWAR machines: a critical review", *Proc. CLAWAR'99*, Portsmouth (1999) pp. 901–910.
6. D. Howard, S.J. Zhang, D.J. Sanger, and S. Miao, "Multi-legged Walker Design – the Joint Torque Versus Workspace Compromise", *Proc. IMechE*, (1997). **211**(C6), pp. 477–488.
7. S.J. Zhang, D. Howard, D.J. Sanger, and S. Miao, "Multi-legged Walking Machine Body Design", *Robotica*, **15**, Part 6, 593–598 (1997).
8. D. Howard, S.J. Zhang, D.J. Sanger, and J.Q. Chen, "Walking Machine Leg Design: The Effect of Leg Geometry on Knee Torque", *Proc. IMechE*, (1999). **213** Part C, pp. 581–590.

https://doi.org/10.1017/S0263574700002861 Published online by Cambridge University Press